



OPEN

CD68- and CD163-positive tumor-associated macrophages in renal clear cell carcinoma

Yingying Yang^{1,3}, Di Sun^{2,3}, Xiaohong Ma¹, Tianqi Wang¹✉ & Jitao Wu¹✉

This study aimed to analyze the infiltration of tumor-associated macrophages (TAMs) in clear cell renal cell carcinoma (ccRCC) and to assess their Prognostic significance. This study involved a Cohort of 106 patients with ccRCC who underwent partial or radical nephrectomy. Immunohistochemistry (IHC) was employed to assess the expression of two distinct types of macrophages at various tissue locations. The diagnostic utility of CD68-positive (CD68⁺) and CD163-positive (CD163⁺) macrophages was determined via Kaplan–Meier with log-rank tests and Multivariable Cox regression. Compared with those in adjacent tissues, the numbers of CD68⁺ and CD163⁺ TAMs were significantly elevated in ccRCC tissues. Kaplan–Meier analysis demonstrated that high CD163⁺ TAM density was significantly associated with poorer overall survival ($p = 0.006$ in tumor nest, $p = 0.043$ in stroma), while CD68⁺ TAMs showed no significant prognostic value ($p > 0.4$ for all comparisons). Multivariable Cox regression confirmed CD163⁺ TAMs as independent prognostic factors after adjusting for tumor size and histological grade, with particularly strong association in tumor stroma (adjusted HR = 7.22, 95% CI 1.06–25.54, $p = 0.003$) compared to tumor nests (adjusted HR = 3.56, 95% CI 1.03–15.56, $p = 0.045$). TAMs, particularly the M2 subtype (CD163⁺), are identified as adverse prognostic factors for ccRCC patients. Those with a high density of M2 macrophages tend to have a poorer prognosis.

Keywords Renal clear cell carcinoma, Tumor-associated macrophages, CD68, CD163, Cellular immunity

Abbreviations

TAMs	Tumor-associated macrophages
ccRCC	Clear cell renal cell carcinoma
IHC	Immunohistochemistry
K-M	Kaplan–Meier
RCC	Renal cell carcinoma
Scr	Serum creatinine
GFR	Glomerular filtration rate
TS	Tumor stroma
TN	Tumor nest
OS	Overall survival
HRs	Hazard ratios

Renal cell carcinoma (RCC) encompasses a spectrum of malignant carcinomas originating from nephrons, with clear cell renal cell carcinoma (ccRCC) being the Most Common type, constituting Approximately 75% of cases^{1,2}. The management of ccRCC has garnered significant attention, with increasing evidence suggesting that the immune response plays a pivotal role in the carcinogenesis of ccRCC and its response to therapy^{3–5}.

Macrophages are potent immune effector cells with remarkable functional adaptability, which has sparked significant interest in exploring their role in cancer immunotherapy. Specifically, the diverse functions of macrophages, both antitumor and protumor, depending on the context, have prompted investigations into their therapeutic potential. Tumor-associated macrophages (TAM) are defined as macrophages located within or in close proximity to the tumor. Macrophages typically exhibit two distinct polarization states: the M1 phenotype, which is known for its proinflammatory and antitumor properties, and the M2 phenotype, which is associated with promoting tumor progression and metastasis^{5,6}. CD68 is a widely recognized marker for

¹Department of Urology, The Affiliated Yantai Yuhuangding Hospital of Qingdao University, NO. 20 East Yuhuangding Road, Yantai 264000, Shandong, China. ²Department of Pathology, The Affiliated Yantai Yuhuangding Hospital of Qingdao University, NO. 20 East Yuhuangding Road, Yantai 264000, Shandong, China. ³Yingying Yang, Di Sun are co-first author. ✉email: weatherking@hotmail.com; wjturology@163.com

macrophages, whereas CD163 serves as a specific marker for M2-type macrophages^{7,8}. In this study, we employed immunohistochemistry (IHC) to assess the distribution and density of CD68⁺ and CD163⁺ macrophages in various regions of tumor tissues from patients with ccRCC.

Our goal was to investigate the potential prognostic significance of these markers in postoperative ccRCC patients, providing insights for clinical application.

Methods and materials

Patients

We Consecutively Collected 366 patients diagnosed with ccRCC WHO underwent surgery at the Department of Urology, Yantai Yuhuangding Hospital of Qingdao University, between January 2015 And December 2017. The inclusion criteria for patients were as follows: (1) Aged 18 years and older, provided informed consent, and voluntarily participated in this study; (2) compliant With the 2010 EAU Guidelines for Renal Cell Carcinoma; (3) had not received any preoperative antitumor therapies such as radiofrequency ablation, chemotherapy or radiation therapy; (4) had undergone either partial nephrectomy or radical nephrectomy, with confirmation by two or more pathologists that the surgical specimens exhibited clean-cut margins and were free from residual ccRCC. The exclusion criteria were as follows: (1) patients with recent infectious diseases or a history of autoimmune diseases or infectious diseases; (2) patients with a history of primary tumors in other organs; (3) patients who had undergone preoperative radiotherapy or chemotherapy; and (4) Individuals WHOse laboratory and pathology data Were incomplete. Following a Rigorous screening Process, A total of 106 ccRCC patients who met the criteria were included in this study. Informed consent was obtained and signed by all participating subjects. Additionally, the study was approved by the Ethics Committee of the Affiliated Yantai Yuhuangding Hospital of Qingdao University (Approval number: 2025-YHD-041). All research activities were conducted strictly in accordance with relevant ethical guidelines and regulations, particularly adhering to the principles of the Declaration of Helsinki, to ensure the rights and safety of the participants were fully protected⁹.

Data collection

After providing informed consent, we conducted face-to-face interviews with the patients. For data collection, we employed the ccRCC Patient Questionnaire (see Appendix I), which was designed by our research team. This questionnaire encompasses a range of inquiries covering general demographic data, health-related details such as smoking and alcohol consumption, medical history, medication history, and various parameters related to the disease, including imaging data, laboratory indicators, surgical information, and pathology reports. During the follow-up period, we recorded a comprehensive set of data, which included various essential parameters, including tumor size (cm), clinical T stage, pathological grade, metastasis, serum creatinine (Scr), and the glomerular filtration rate (GFR). Our follow-up strategy involved rigorous monitoring of patient health. Post surgery, the first follow-up occurred every three months during the initial two years, followed by biannual follow-ups for the subsequent two years and, finally annual check-ups in the previous year. These follow-up sessions included a detailed medical history, physical examination, laboratory blood tests, imaging assessments, and cases of patient fatality, WHich Were obtained through telephone interviews. The follow-up Period Was until January 10, 2022. All experiments involving humans and/or the use of human tissue samples in this study were conducted in strict accordance with the Ethics Committees.

IHC staining of tissue samples

Tissue samples were collected from both the tumor and adjacent nontumor areas of the included patients. These excised samples were promptly preserved in liquid nitrogen and subsequently transferred to a -80 °C refrigerator. For further analysis, we performed H&E staining. The primary antibodies used were anti-CD68 rabbit monoclonal antibody (dilution 1:500) (Absin, China) and anti-CD163 rabbit monoclonal antibody (1:500) (Absin, China), and the secondary antibody used was goat anti-rabbit IgG (1:500) (Absin, China).

Following staining, two certified pathologists performed manual quantitative analysis of macrophages without access to any clinical data. We employed the hotspot method, with the following steps: (1) First, each slide was scanned at low magnification (100×) to identify five regions with the highest density of positively stained cells (hotspots); (2) Using an Olympus BX53 microscope equipped With the Cell Sens Standard 2.3 counting module (Olympus Corporation, Japan), CD68⁺ and CD163⁺ cells Within each Hotspot area were Counted separately At 400× magnification; (3) The final density for each marker was obtained by calculating the average count value of the five hotspot regions and expressed in cells/mm².

To ensure inter-observer consistency, two Pathologists underwent Pre-training using 20 representative images (10 CD68⁺ And 10 CD163⁺) prior to the study to standardize counting criteria (e.g., membrane/cytoplasmic staining thresholds, exclusion of necrotic areas, etc.). If inter-observer differences exceeded 15%, joint review was conducted until consensus was reached. Intraclass correlation coefficients (ICCs) Were calculated For 30 randomly selected samples, showing high consistency (CD68⁺ ICC = 0.87, 95% CI 0.82–0.91; CD163⁺ ICC = 0.89, 95% CI 0.85–0.93).

Statistics

Spearman's Rho and χ^2 tests were employed to compare the expression levels of CD68 and CD163 with patient and tumor characteristics. Kaplan-Meier analysis, along with log-rank tests, was used to determine differences in overall survival (OS) based on CD163 and CD68 expression. Additionally, we utilized Cox regression proportional hazards models to estimate hazard ratios (HRs) for death, considering both uni- and multivariate analyses. Covariates with a p value ≤ 0.05 in the univariate analysis were included in the multivariate analysis. All the statistical tests were two-sided, and significance was determined at $p \leq 0.05$. The statistical analyses Were Performed via IBM SPSS Statistics 25 (IBM, Armonk, NY, USA).

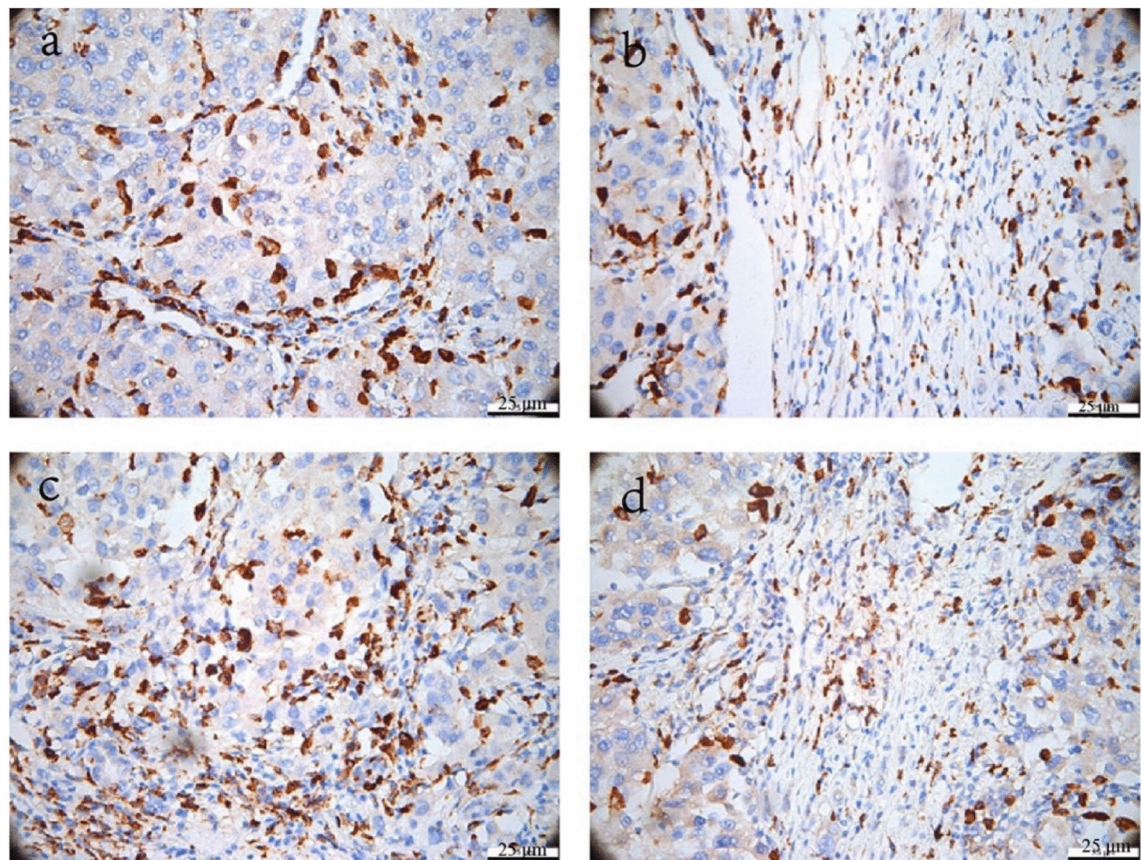


Fig. 1. Immunohistochemical staining of CD68⁺ tumor-associated macrophages (TAMs) and CD163⁺ tumor associated macrophages (TAMs) in ccRCC. Representative images of high-density CD68⁺ staining (**a, b**) and CD163⁺ staining (**c, d**) in the tumor stroma and tumor nest. (Original magnification, $\times 200$).

Variables	Mean	SD	Median	Range
CD68 ⁺ TAM Tumor nest	31.55	18.84	26.2	8.8–117.2
Tumor stroma	21.13	11.27	16.3	5.6–57
CD163 ⁺ TAM Tumor nest	28.49	17.76	23.0	4.8–95
Tumor stroma	18.53	10.01	16.6	2.6–54.4
Ratio of CD163 and CD68 Tumor nest	0.92	0.26	0.91	0.32–1.68
Tumor stroma	0.95	0.21	0.94	0.52–1.49

Table 1. Clinicopathological features of ccRCC and the status of TAMs.

Results

We measured the expression levels of CD68 and CD163 in both the TSs And TNs of All 106 samples. Our analysis revealed the presence of CD68⁺ (Fig. 1a, b) and CD163⁺ (Fig. 1c, d) macrophages in both the TS and TN of the TNC. The relationships between TAM density (CD68⁺ or CD163⁺) and clinicopathological features are presented in Table 1. The cutoff values Were as Follows: 16.3 for CD68 in the TS, 26.2 for CD68 in the TN, 16.6 for CD163 in the TS, And 23.0 for CD163 in the TN. Additionally, for the CD163/CD68 ratios, the cutoff values Were 0.91 For TN And 0.94 for TS. (Table 2). Our research revealed significant correlations between high CD68⁺ TAM density in both the TS and TN and several clinical factors. Notably, it was significantly correlated with larger tumor size ($p < 0.001$). Furthermore, the high density of CD163⁺ TAMs in TS patients was significantly correlated with older age ($p = 0.031$), although this correlation was not observed in TNs ($p = 0.310$). In addition, both high CD68⁺ TAM and CD163⁺ TAM densities in the TS and TN were associated with higher histological grade ($p < 0.001$), larger tumor size ($p < 0.001$), and lymph node metastasis ($p < 0.001$). Conversely, no significant correlation was observed between the number of TAMs (CD68⁺ or CD163⁺ cells and the CD163/CD68 ratio) and patient sex in the TS or TN. However, the CD163/CD68 ratio in TS patients was correlated with patient

Clinicopathological features	CD68						CD163						CD163/CD68					
	Tumor nest			Tumor stroma			Tumor nest			Tumor stroma			Tumor nest			Tumor stroma		
	Low	High	P value	Low	High	P value	Low	High	P value	Low	High	P value	Low	High	P value	Low	High	P value
Age (years)			<0.001			<0.001			0.031			0.310			0.011			0.121
≤63	23	31		18	36		24	30		25	29		21	33		23	31	
>63	42	10		45	7		34	18		19	33		33	19		30	22	
Gender			0.821			0.239			0.349			0.368			0.084			0.449
Male	43	28		36	35		42	29		36	35		34	37		35	36	
Female	22	13		22	13		24	11		21	14		23	12		20	15	
Tumor size (cm)			<0.001			<0.001			<0.001			<0.001			0.012			0.501
≤5	53	4		46	11		55	2		47	10		36	21		30	27	
>5	12	37		12	37		9	40		10	39		19	30		29	20	
Histological grade			<0.001			<0.001			<0.001			<0.001			0.195			0.320
I - II	54	24		52	26		53	25		54	24		39	39		42	36	
III - IV	11	17		1	27		2	26		1	27		10	18		12	16	
Lymph node metastasis			0.001			0.034			0.009			0.006			0.132			0.642
No	64	33		57	40		64	33		57	40		50	47		51	46	
Yes	1	8		2	7		2	7		1	8		7	2		4	5	
Mortality			0.054			0.135			0.003			0.014			0.166			0.166
No	63	36		57	42		69	30		61	38		55	44		55	44	
Yes	2	5		2	5		1	6		1	6		2	5		2	5	

Table 2. Distribution pattern of TAMs in ccRCC. (TAMs, tumor-associated macrophages; ccRCC, clear cell renal cell carcinoma; SE, standard error) clear cell renal cell carcinoma; SE, standard error).

age ($p=0.012$) and tumor size ($p=0.012$). No such correlations were found with other clinical and pathological features. We further conducted univariate and multivariate Cox regression analyses to examine the impact of clinicopathological prognostic factors and the expression of CD68 and CD163 on OS (Table 3). Multivariate Cox regression analysis revealed that CD163⁺ TAMs in the TS and TN were strongly correlated with patient OS (HR = 7.22, 95% CI 1.06–25.54, $p=0.003$; HR = 3.56, 95% CI 1.03–15.56, $p=0.045$). K-M analysis and the log-rank test were used to compare the expression status and survival rates associated with different TAMs. A higher density of CD68⁺ TAMs in the TN was not correlated with OS ($p=0.819$). However, a greater density of CD163⁺ TAMs in the TN was significantly correlated with OS ($p=0.006$), whereas a greater CD68⁺/CD163⁺ ratio in the TN was not correlated with OS ($p=0.084$) (Fig. 2a, c, e). In TS, a greater density of CD68⁺ TAMs in the TS was not correlated with OS ($p=0.433$), whereas a greater density of CD163⁺ TAMs in the TS was significantly correlated with OS ($p=0.043$). Similarly, a higher CD68⁺/CD163⁺ ratio in the TS was not correlated with OS ($p=0.738$) (Fig. 2b, d, f).

Discussion

As crucial components of innate immunity, macrophages, which are known to infiltrate tumor tissues, adapt their function on the basis of specific tumor microenvironments^{10,11}. This adaptation leads to different polarization states, where macrophages can assume distinct roles depending on their polarization type. Specifically, TAMs are macrophages found within or near tumor tissues and are known to polarize into two subgroups: the M1 phenotype and the M2 phenotype. To distinguish and study these macrophage subtypes, CD68 serves as a universal marker of macrophages, whereas CD163 can be used to identify M2-type macrophages^{10,12}. In this study, We explored the Relationship between Macrophages and ccRCC. We analyzed data From 106 patients who had undergone surgical treatment for ccRCC. Using immunohistochemistry, we assessed the distribution and density of CD68⁺ and CD163⁺ macrophages within various regions of ccRCC tumor tissues. Furthermore, we conducted survival analysis to better understand the implications of the presence of macrophages in ccRCC.

In this study, we observed that both intra- and paraneoplastic tissues contained a greater number of CD68⁺ macrophages than CD163⁺ macrophages. Additionally, there was a significant positive correlation between the quantity of CD68⁺ macrophages and the number of CD163⁺ macrophages in both renal cancer tissues and the tumor stroma. This correlation aligns with the well-established fact that the total population of macrophages is more abundant than M2-like macrophages are, and CD163 serves as a specific marker for the latter. Through data analysis, we found that macrophage infiltration was notably greater within cancerous tissue. Consequently, CD68/CD163 expression levels are significantly elevated in cancer tissues compared with those in the tumor stroma. This finding is consistent with several recent preclinical studies in various solid tumors (pancreatic, breast, ovarian, gastric, bladder, ovarian, and thyroid cancers). These studies have consistently demonstrated the tumor-promoting function of TAMs^{7,13–15}. Notably, some researchers have proposed different results from ours. For example, Ren et al. reported that CD68 expression in hepatocellular carcinoma tissues was greater than that in paraneoplastic tissues and was associated with lymph node metastasis and the pathological stage of liver cancer tissues¹⁶. This variance in findings might be attributed to the heterogeneous nature of macrophages in hepatocellular carcinoma, including the presence of Kupffer cells. Additionally, differences in study methodologies, sample types, or clinicopathological characteristics of patients could contribute to these discrepancies^{17,18}.

In our study, we selected three key indicators: CD68⁺ TAMs, CD163⁺ TAMs, and the CD163/CD68 ratio. When univariate prognostic analysis was conducted, we found a significant correlation between CD163⁺ TAMs in cancer tissue and postoperative OS. Specifically, patients with lower CD163⁺ TAM density tended to have a better prognosis. However, no significant correlations were detected between CD68⁺ TAMs and the CD68/CD163 ratio. These findings suggest that the M2 subtype of macrophages within TAMs predominantly affects

Clinicopathological features	Univariate analysis		Multivariate analysis	
	OS HR (95% CI)	P value	OS HR (95% CI)	P value
Age (≤ 63 vs. > 63)	3.66 (0.38–5.28)	0.260		
Gender (Male vs. Female)	1.05 (0.61–7.91)	0.965		
Tumor size (≤ 5 cm vs. > 5 cm)	3.99 (0.41–8.39)	0.231		
Histological grade (I - II vs. III-IV)	2.89 (0.32–4.30)	0.990		
Lymph node metastasis (No vs. Yes)	4.62 (1.41–7.27)	0.982		
TN CD68 (low vs. high)	3.21 (0.11–21.64)	0.416		
TS CD68 (low vs. high)	4.33 (0.33–65.47)	0.752		
TN CD163 (low vs. high)	7.57 (1.83–28.80)	0.035	7.21 (1.05–25.54)	0.037
TS CD163 (low vs. high)	3.78 (1.13–16.47)	0.041	3.55 (1.03–15.55)	0.045
TN CD163/CD68 (low vs. high)	3.02 (0.11–13.33)	0.135		
TS CD163/CD68 (low vs. high)	0.99 (0.10–3.38)	0.755		

Table 3. Univariate and multivariate Cox regression analyses for overall survival (OS) in patients with ccRCC. (OS, overall survival. HR hazard ratio, CI confidence interval, TS tumor stroma, TN tumor nest, *p value is significant).

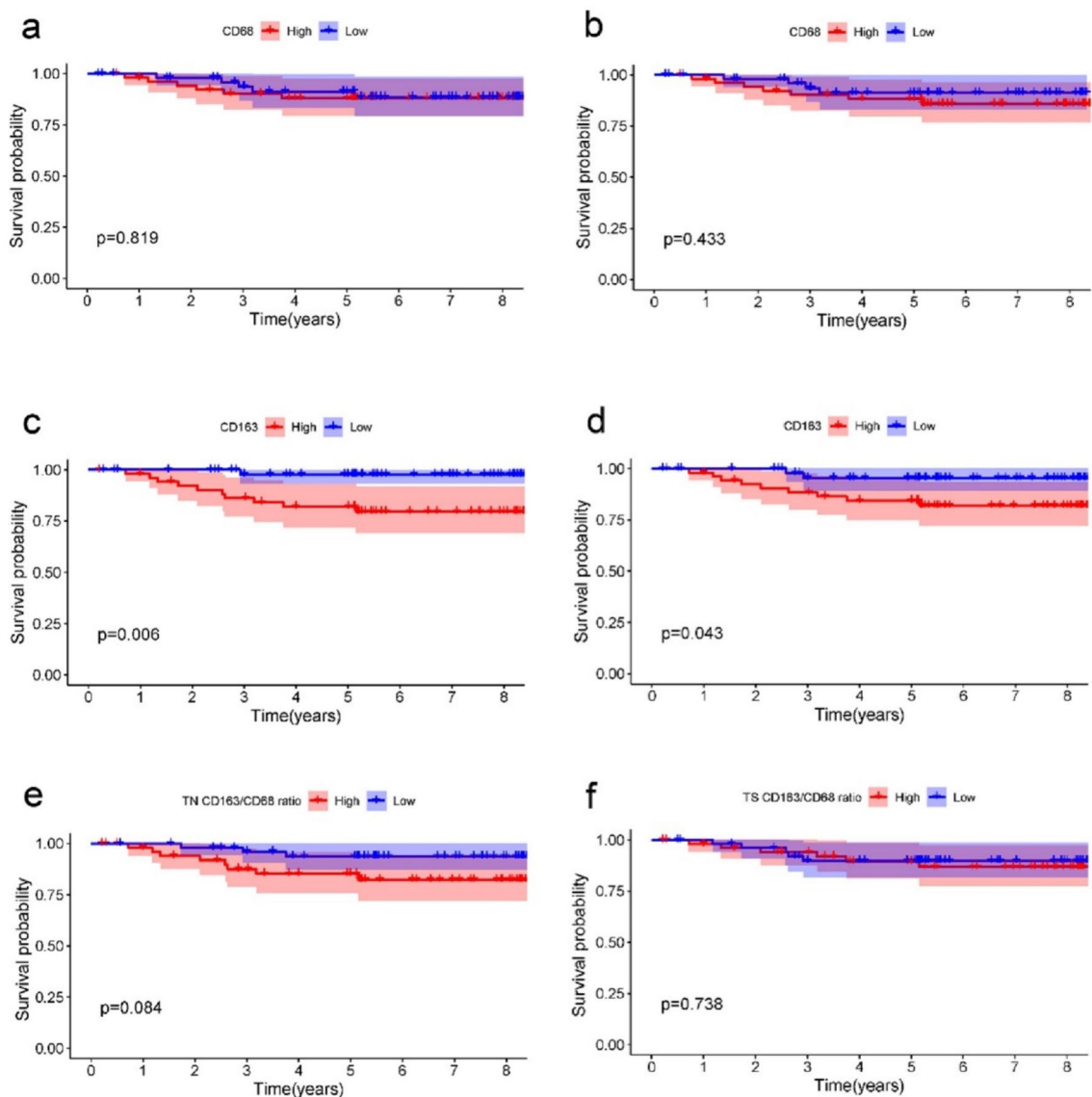


Fig. 2. Prognostic significance of TAMs in clear cell renal cell carcinoma (ccRCC). The Kaplan–Meier curves for overall survival (OS) were stratified by the median values as the cutoff for prognostic evaluation and divided into low- or high-TAM variable subsets. CD68⁺ TAMs did not demonstrate prognostic significance for OS (a, b) in the tumor stroma (TS) or tumor nest (TN). A high density of CD163⁺ TAMs in the TS and TN was associated with poor RFS and OS (c, d). OS (e, f) curves according to the infiltration density of the CD163⁺/CD68⁺ ratio in TSs and TNs.

patient prognosis. Furthermore, the M2 subtype of macrophages, which serves as a risk factor, has substantial prognostic value in this context.

In current clinical applications of macrophage immunotherapy models, the primary strategies focus on either reducing TAMs or transforming TAMs from the M2 tumor-promoting phenotype to the M1 antitumor phenotype¹⁹. One promising approach involves the use of CSF-1R inhibitors that specifically target TAMs. These inhibitors have demonstrated their ability to impede malignant progression. Several selective CSF-1R (or M-CSF) inhibitors are currently undergoing clinical studies. These inhibitors include antibody drugs such as axatilimab, emactuzumab, and cabiralizumab, as well as small-molecule drugs such as pimicotinib, vimseltinib, and evicotinib. They function by blocking CSF-1 signaling, leading to a reduction in TAMs, which in turn has shown promise in improving patient prognosis^{20,21}.

Many studies have shown that increased CD163 expression is associated with increased proliferation and metastatic potential in various solid tumors^{14,15}. Our IHC results and data analysis align with this trend, suggesting that the prognostic impact of TAM density primarily hinges on M2-subtype macrophages. These findings underscore the significant prognostic relevance of M2 macrophages in ccRCC. However, leveraging TAMs for therapeutic purposes presents a challenge because of their widespread distribution in the body and their key role in innate immunity. Achieving specific targeting of M2 TAMs has remained a formidable research

hurdle^{22,23}. Currently, clinical therapies targeting M2 TAMs are limited and predominantly focus on CD163^{24,25}. A notable breakthrough has been made by Professor Dongfang Zhou's team, who devised and synthesized a hemoglobin-poly(ϵ -caprolactone) (Hb-PCL)-conjugated polymer²⁶. This innovative compound selectively targets M2 macrophages via CD163 surface receptors. It has demonstrated efficacy in inhibiting tumor metastasis and recurrence and significantly reduces the toxicity associated with small molecule drugs. This was observed in both a murine breast cancer metastasis model (4T1) and a postoperative recurrence model of subcutaneous murine colon cancer (CT26). Additionally, itaconic acid and its derivative Octyl Itaconate have been found to block M2 polarization by inhibiting the JAK1/STAT6 signaling pathway downstream of IL-4. Furthermore, by directly targeting JAK1, itaconic acid and OI have been identified as JAK1 inhibitors. They hold Promise For the treatment of type 2 immune-mediated diseases, including allergies, asthma and fibrosis^{27–29}. Moreover, Peng et al. highlighted the potential of miR-136 to inhibit M2 macrophage polarization by suppressing CD163 transcription. These developments in tumor immunomodulation hold great promise^{27–29}.

While previous studies have established the prognostic role of CD68⁺ and CD163⁺ TAMs in ccRCC^{30,31}, our study advances this field by demonstrating the compartment-specific distribution and clinical significance of these macrophages. Earlier works primarily assessed TAMs as a bulk population within entire tumor sections, potentially masking critical spatial heterogeneity. Our spatial analysis revealed that CD163⁺ TAMs in the TS exhibited a stronger association with poor overall survival (HR = 7.22, $p = 0.003$) compared to those in TN (HR = 3.56, $p = 0.045$), suggesting that M2 macrophage-mediated immunosuppression may be more active in the stromal microenvironment. This compartmentalized pattern aligns with recent findings in breast cancer³² but has not been rigorously validated in ccRCC. Our data further highlight that the CD163⁺/CD68⁺ ratio in TS, but not TN, correlated with tumor size ($p = 0.012$), implying distinct biological roles of TAM subsets in different niches. Mechanistically, M2-polarized TAMs in the stroma may facilitate tumor progression through multiple pathways: (1) Secretion of VEGF and MMP-9 to promote angiogenesis and extracellular matrix remodeling^{33,34}; (2) Recruitment of regulatory T cells via CCL22/CCL18, fostering an immunosuppressive microenvironment³⁵; (3) Metabolic support via lactate shuttle, enhancing tumor cell survival under hypoxic conditions³⁶. Notably, the spatial specificity of CD163⁺ TAMs in TS (HR = 7.22) suggests their dominant role in stromal-mediated immune evasion, which aligns with recent findings in breast cancer³². These observations underscore the potential of stromal-targeted therapies, such as CSF-1R inhibition, to disrupt TAM-mediated protumor networks in ccRCC³⁷.

While our study provides valuable insights, it has certain limitations. This study used tumor diameter rather than T staging, which may limit direct comparisons with staging-based prognostic systems. However, our size-based stratification (including the AJCC 7 cm cutoff value) and multivariate adjustment alleviated this concern, particularly for local disease. Future studies should incorporate microscopic invasion status (e.g., renal pelvis involvement) to refine T stage assessment. This study used OS as the primary endpoint. The lack of standardized recurrence monitoring precludes analysis of DFS or the role of TAMs in early treatment failure. Prospective studies with standardized imaging follow-up protocols (CT/MRI every 3–6 months) are needed to address this gap.

Conclusion

Our study sought to examine the prognostic value of TAMs in ccRCC. These findings indicate that the infiltration of M2 TAMs (CD163⁺) is a significant risk factor for ccRCC patients. Those with a high density of M2 TAMs may have a poorer prognosis. These results emphasize the importance of considering macrophage subtypes in ccRCC prognosis and treatment planning.

Data availability

All data generated or analyzed during this study are included in this published article.

Received: 4 March 2025; Accepted: 5 September 2025

Published online: 08 October 2025

References

1. R, J. et al. Characteristics of clear cell papillary renal cell carcinoma (ccpRCC). *Int. J. Mol. Sci.* **23**(1), 151 (2021).
2. R, F. L. et al. Prognostic gene expression-based signature in clear-cell renal cell carcinoma. *Cancers* **14**(15), 3754 (2022).
3. WH, X. et al. Prognostic value and immune infiltration of novel signatures in clear cell renal. *Aging* **11**(17), 6999–7020 (2019).
4. L, Y. et al. The tumour microenvironment and metabolism in renal cell carcinoma targeted or immune therapy. *J. Cell Physiol.* **236**(3), 1616–1627 (2021).
5. A, N. R. et al. Macrophage-based approaches for cancer immunotherapy. *Cancer Res.* **81**(5), 1201–1208 (2021).
6. S-M, A. et al. Macrophage plasticity, polarization, and function in health and disease. *J. Cell Physiol.* **233**(9), 6425–6440 (2018).
7. H, J. M. et al. CD163 as a marker of M2 macrophage, contribute to predict aggressiveness and prognosis of Kazakh esophageal squamous cell carcinoma. *Oncotarget* **8**(13), 21526–21538 (2017).
8. P, Y. et al. Tumor-associated macrophages in tumor immunity. *Front. Immunol.* **11**, 583084 (2020).
9. World Medical Association Declaration of Helsinki. Ethical principles for medical research involving human participants. *JAMA* **333**(1), 71–74 (2025).
10. Witjes, J. A. et al. European association of urology guidelines on muscle-invasive and metastatic bladder cancer: Summary of the 2020 guidelines. *Eur. Urol.* **79**(1), 82–104 (2021).
11. X, R. et al. Liver tumour immune microenvironment subtypes and neutrophil heterogeneity. *Nature* **612**(7938), 141–147 (2022).
12. Patel, V. G., Oh, W. K. & Galsky, M. D. Treatment of muscle-invasive and advanced bladder cancer in 2020. *CA Cancer J. Clin.* **70**(5), 404–423 (2020).
13. Wang, N., Liang, H. & Zen, K. Molecular mechanisms that influence the macrophage m1–m2 polarization balance. *Front. Immunol.* **5**, 614 (2014).
14. C, Y. et al. Tumor-recruited M2 macrophages promote gastric and breast cancer metastasis via M2 macrophage-secreted CHI3L1 protein. *J. Hematol. Oncol.* **10**(1), 017–0408 (2017).

15. F, S. M. et al. Immune and inflammatory cells in thyroid cancer microenvironment. *Int. J. Mol. Sci.* **20**(18), 4413 (2019).
16. R, C. X. et al. Intratumoral and peritumoral expression of CD68 and CD206 in hepatocellular. *Oncol. Rep.* **38**(2), 886–898 (2017).
17. H, H. et al. The role of macrophage TAM receptor family in the acute-to-chronic progression of liver disease: From friend to foe?. *Liver Int.* **42**(12), 2620–2631 (2022).
18. H, V. et al. Intrinsic and extrinsic control of hepatocellular carcinoma by TAM receptors. *Cancer* **13**(21), 5448 (2021).
19. L, Y., J, X. & H, L. Tumor-associated macrophages in tumor metastasis: Biological roles and clinical. *J. Hematol. Oncol.* **12**(1), 019–0760 (2019).
20. Pyontec, S. M. et al. CSF-1R inhibition alters macrophage polarization and blocks glioma progression. *Nat. Med.* **19**(10), 1264–1272 (2013).
21. H, D. A. & KP, M. Therapeutic applications of macrophage colony-stimulating factor-1 (CSF-1) and antagonists of CSF-1 receptor (CSF-1R) signaling. *Blood* **119**(8), 1810–1820 (2012).
22. L-Y, M. et al. Macrophage targeting in cancer. *Ann. N. Y. Acad. Sci.* **1499**, 18–41 (2021).
23. X, Y. et al. Engineering macrophages for cancer immunotherapy and drug delivery. *Adv. Mater.* **32**(40), e2002054 (2020).
24. M, D. et al. Myeloid cell-targeted STAT3 inhibition sensitizes head and neck cancers to radiotherapy and T cell-mediated immunity. *J. Clin. Invest.* **131**(2), e137001 (2021).
25. Rashki, S. et al. Delivery LL37 by chitosan nanoparticles for enhanced antibacterial and antibiofilm efficacy. *Carbohydr Polym* **291**, 119634 (2022).
26. W, Y. et al. Engineering endogenous tumor-associated macrophage-targeted biomimetic nano-RBC to reprogram tumor immunosuppressive microenvironment for enhanced chemo-immunotherapy. *Adv. Mater* **33**(39), e2103497 (2021).
27. R, M. C. et al. Itaconate and itaconate derivatives target JAK1 to suppress alternative. *Cell Metab.* **34**(3), 487–501 (2022).
28. X, H. et al. Injectable hydrogel loaded with 4-octyl itaconate enhances cartilage regeneration. *Biomater Sci.* **11**(7), 2445–2460 (2023).
29. C, K. V. et al. Octyl gallate induces pancreatic ductal adenocarcinoma cell apoptosis and and suppresses endothelial-mesenchymal transition-promoted M2-macrophages, hsp90 α secretion, and tumor growth. *Cell* **9**(1), 91 (2019).
30. Anno, T. et al. Prognostic role of the innate immune signature CD163 and “eat me” signal calreticulin in clear cell renal cell carcinoma. *Cancer Immunol. Immunother.* **72**(6), 1779–1788 (2023).
31. Chakiryan, N. H. et al. Spatial clustering of CD68+ tumor associated macrophages with tumor cells is associated with worse overall survival in metastatic clear cell renal cell carcinoma. *PLoS ONE* **16**(4), e0245415 (2021).
32. Jamiyan, T. et al. CD68- and CD163-positive tumor-associated macrophages in triple negative cancer of the breast. *Virchow. Arch* **477**(6), 767–775 (2020).
33. Lai, Y. S. et al. Autocrine VEGF signalling on M2 macrophages regulates PD-L1 expression for immunomodulation of T cells. *J. Cell Mol. Med.* **23**(2), 1257–1267 (2019).
34. Tian, K. et al. MMP-9 secreted by M2-type macrophages promotes Wilms' tumour metastasis through the PI3K/AKT pathway. *Mol. Biol. Rep.* **49**(5), 3469–3480 (2022).
35. Mortazavi Farsani, S. S. et al. Pyruvate kinase M2 activation reprograms mitochondria in CD8 T cells, enhancing effector functions and efficacy of anti-PD1 therapy. *Cell Metab.* **37**(6), 1294–1310.e7 (2025).
36. Kang, B. S. et al. Effects of pyruvate kinase M2 (PKM2) Gene deletion on astrocyte-specific glycolysis and global cerebral ischemia-induced neuronal death. *Antioxidants (Basel)* **12**(2), 491 (2023).
37. Yang, L. et al. High expression of colony-stimulating factor 1 receptor associates with unfavorable cancer-specific survival of patients with clear cell renal cell carcinoma. *Ann. Surg. Oncol.* **23**(3), 1044–1052 (2016).

Author contributions

Conceptualization: Jitao Wu. Data curation: Yingying Yang, Tianqi Wang. Formal analysis: Yingying Yang, Tianqi Wang. Funding acquisition: Jitao Wu. Investigation: Yingying Yang, Xiaohong Ma. Methodology: Yingying Yang, Tianqi Wang, Xiaohong Ma. Project administration: Jitao Wu. Resources: Yingying Yang, Tianqi Wang, Di Sun. Software: Yingying Yang, Tianqi Wang, Di Sun. Supervision: Jitao Wu. Writing original draft: Yingying Yang. Writing review & editing: Jitao Wu.

Funding

This work was supported by the National Natural Science Foundation of China (Nos. 82370690), Natural Science Foundation of Shandong Province (Nos. ZR2023MH241), and Taishan Scholars Program of Shandong Province (Nos. tsqn201909199).

Declarations

Competing interests

The authors declare no competing interests.

Ethics

The studies involving human participants were reviewed and approved by the ethics committee of the affiliated Yantai Yuhuangding hospital of Qingdao university. The patients/participants provided their written informed consent to participate in this study.

Consent for publication

The authors warranted that their paper is original and had full authority to give this consent. All data generated or analyzed during this study are included in this published article.

Additional information

Supplementary Information The online version contains supplementary material available at <https://doi.org/10.1038/s41598-025-19003-9>.

Correspondence and requests for materials should be addressed to T.W. or J.W.

Reprints and permissions information is available at www.nature.com/reprints.

Publisher's note Springer Nature remains neutral with regard to jurisdictional claims in published maps and institutional affiliations.

Open Access This article is licensed under a Creative Commons Attribution-NonCommercial-NoDerivatives 4.0 International License, which permits any non-commercial use, sharing, distribution and reproduction in any medium or format, as long as you give appropriate credit to the original author(s) and the source, provide a link to the Creative Commons licence, and indicate if you modified the licensed material. You do not have permission under this licence to share adapted material derived from this article or parts of it. The images or other third party material in this article are included in the article's Creative Commons licence, unless indicated otherwise in a credit line to the material. If material is not included in the article's Creative Commons licence and your intended use is not permitted by statutory regulation or exceeds the permitted use, you will need to obtain permission directly from the copyright holder. To view a copy of this licence, visit <http://creativecommons.org/licenses/by-nc-nd/4.0/>.

© The Author(s) 2025